AD-A141 869   ZINC SELENIDE PHOTOELECTRODES EFFICIENT RADIATIVE          1/1
              RECOMBINATION IN A STAB..(U) WISCONSIN UNIV-MADISON
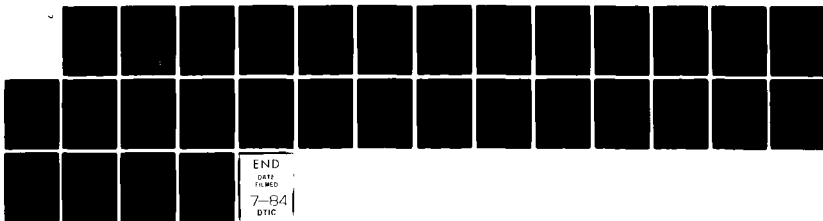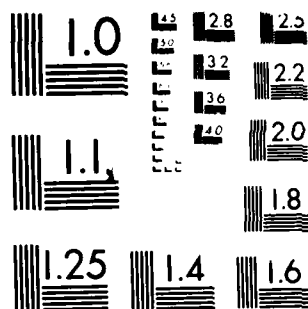              DEPT OF CHEMISTRY  P M SMILEY ET AL. 25 MAY 84
UNCLASSIFIED  UWIS/DC/TR-84/1 N00014-78-C-0633          F/G 10/2      NL

END
DATE
FILMED
7-84
DTIC

MICROCOPY RESOLUTION TEST CHART

NATIONAL BUREAU OF STANDARDS 1963 A

Zinc Selenide Photoelectrodes. Efficient Radiative Recombination
in a Stable Photoelectrochemical Cell

by

Patricia M. Smiley, Richard N. Biagioni, and Arthur B. Ellis

Prepared for Publication

in

Journal of the Electrochemical Society

Department of Chemistry
University of Wisconsin
Madison, Wisconsin 53706

May 25, 1984

DTIC
SELECTED
JUN 0 7 1984

E

84  06  06  006

| REPORT DOCUMENTATION PAGE | | READ INSTRUCTIONS BEFORE COMPLETING FORM |
|---|---|---|
| 1. REPORT NUMBER<br>UWIS/DC/TR-84/1 | 2. GOVT ACCESSION NO.<br>AD-A141869 | 3. RECIPIENT'S CATALOG NUMBER |
| 4. TITLE (and Subtitle)<br>Zinc Selenide Photoelectrodes. Efficient Radiative Recombination in a Stable Photoelectrochemical Cell | | 5. TYPE OF REPORT & PERIOD COVERED |
| | | 6. PERFORMING ORG. REPORT NUMBER |
| 7. AUTHOR(s)<br>Patricia M. Smiley, Richard N. Biagioni, and Arthur B. Ellis | | 8. CONTRACT OR GRANT NUMBER(s)<br>N00014-78-C-0633 |
| 9. PERFORMING ORGANIZATION NAME AND ADDRESS<br>Department of Chemistry, University of Wisconsin, Madison, Wisconsin 53706 | | 10. PROGRAM ELEMENT, PROJECT, TASK AREA & WORK UNIT NUMBERS<br>NR 051-690 |
| 11. CONTROLLING OFFICE NAME AND ADDRESS<br>Office of Naval Research/Chemistry Program Arlington, Virginia 22217 | | 12. REPORT DATE<br>May 25, 1984 |
| | | 13. NUMBER OF PAGES<br>22 |
| 14. MONITORING AGENCY NAME & ADDRESS(If different from Controlling Office) | | 15. SECURITY CLASS. (of this report) |
| | | 15a. DECLASSIFICATION/DOWNGRADING SCHEDULE |

16. DISTRIBUTION STATEMENT (of this Report)

Approved for Public Release: Distribution Unlimited

17. DISTRIBUTION STATEMENT (of the abstract entered in Block 20, if different from Report)

18. SUPPLEMENTARY NOTES

Prepared for publication in the Journal of the Electrochemical Society

19. KEY WORDS (Continue on reverse side if necessary and identify by block number)

photoluminescence, electroluminescence, zinc selenide electrodes, photoelectrochemistry

20. ABSTRACT (Continue on reverse side if necessary and identify by block number)

Photoluminescence (PL) and electroluminescence (EL) from single-crystal, n-type, Al-doped ZnSe (ZnSe:Al) electrodes have been studied. These samples exhibit both edge emission ($\lambda_{max} \sim 460$ nm) and subband gap emission when excited at several ultraband-gap wavelengths. The latter PL band is particularly intense, with a measured radiative quantum yield of $\sim 10^{-1}$ to $10^{-2}$; the transition seems at least partially self-activated (SA) in origin, based on previously reported PL data. Excited-state communication involving the

two emissive states is inferred from time-resolved PL measurements. Stable
photoelectrochemical cells (PEC's) can be constructed from n-ZnSe:Al
electrodes and aqueous diselenide or ditelluride electrolytes. Applied
potential quenches both of the photoanodes' PL bands roughly in parallel.
The extent of PL quenching is consistent with a dead-layer model previously
used to describe quenching in Au-ZnSe Schottky diodes. When used as
a dark cathode in aqueous, alkaline peroxydisulfate electrolyte, EL from
ZnSe:Al electrodes is observed. PL and EL spectral distributions are
similar and indicate that the same emissive excited states are populated
in the two experiments. Measured EL efficiencies, $\sim 10^{-4}$ to $10^{-6}$ at -2.2 and
-1.8 V vs. SCE, respectively, are much smaller than PL efficiencies. Possible
sources of the discrepancies are discussed.

| Accession For | |
|---|---|
| NTIS GRA&I | ☒ |
| DTIC TAB | ☐ |
| Unannounced | ☐ |
| Justification | |
| By | |
| Distribution/ | |
| Availability Codes | |
| Dist | Avail and/or Special |
| A-1 | |

Keen interest in photoelectrochemical cells (PEC's) has focused attention on the excited-state properties of the semiconductor electrodes which serve as the key element of these devices (1). We and others have studied photoluminescence (PL) and electroluminescence (EL) from a variety of II-VI and III-V semiconductor electrodes in an effort to determine the effect of PEC parameters on the solids' excited-state deactivation routes (2). In general, measured radiative quantum yields, $\phi_r$, of these materials have been small, $\sim 10^{-3}$-$10^{-5}$. We describe in this paper an electrode, n-ZnSe:Al, whose emission competes very favorably ($\phi_r \sim 10^{-1}$-$10^{-2}$) with other deactivation paths in stable, efficient PEC's. As observed with other semiconductor electrodes (3), the PL of n-ZnSe:Al electrodes can be perturbed and EL initiated by interfacial charge-transfer processes. We show that PL quenching by applied potential is compatible with a dead-layer model used to describe such quenching in other PEC's (4,5) and in Au-ZnSe Schottky diodes (6).

## Experimental

Materials. Single-crystal (111) plates of n-type ZnSe:Al ($\sim 2$ ppm Al based on arc emission spectroscopy) were generously provided by North American Philips Corp., Briarcliff Manor, N.Y.; the samples ($\sim 5 \times 5 \times 0.25$ mm) had been cut from boules which were obtained from Eagle-Picher Industries, Miami, OK and had been subsequently heat-treated in molten Zn at 950°C for 24 h to lower their resistivity to $\sim 1$-10 ohm-cm. Twinned areas may be present below the surface in some of the samples employed. Sample carrier concentrations of $\sim 10^{17}$-$10^{18}$ cm$^{-3}$ were estimated from both dc Hall measurements (7) and Mott-Schottky data. In the former measurement, a Varian Associates Model V-2301-A dc electromagnet producing a field of $\sim 0.5$ kG was employed. Capacitance measurements of the ZnSe:Al electrodes were made at 1.0 and 0.8 kHz in 1M OH$^-$ and diselenide electrolytes, respectively, using an Ithaco Dynatrac 391 lock-in voltmeter, EG&G PAR Models 173 potentiostat and 175 programmer, and a Wavetek Model 182A 4MHz function generator. Electrodes were prepared by etching the solids for 20 s with 1:40 Br$_2$/MeOH (v/v), making ohmic contact to the Se-rich crystal face by soldering with In, and then mounting the solid as an electrode as described previously (8).

Resistivity in some samples was deliberately enhanced by heat-treatment with Se (Alfa; m3N purity). For these experiments, an $\sim$10-mg sample of ZnSe:Al was placed in a quartz tube with $\sim$0.2 mg of Se. The quartz ampule was evacuated ($\sim$0.1 Torr), sealed to a volume of $\sim$3 cm$^3$, and heated at 700°C in a Lindberg furnace for $\sim$30 s. After its removal from the ampule, the solid was etched until bright PL was observed, then mounted as an electrode. Sulfide, diselenide and ditelluride electrolytes were prepared as described previously (9,10), except that after the solid $Na_2Se$ was washed with NaOH, it was dissolved in conc. KOH to yield solutions whose compositions were $\sim$10M KOH/0.25M Se$^{2-}$. During PEC experiments, the electrolytes were vigorously stirred and blanketed with $N_2$. Preparation of peroxydisulfate electrolyte has been described (11). MgO powder was obtained from Baker Chemical Co.

PL Properties. Front-surface PL spectra at ambient temperature and at 77 K were obtained with the Aminco-Bowman spectrophotofluorometer described previously (3). The high-pressure Xe lamp of the instrument was used in conjunction with an interference filter (Edmund Scientific) for 405-nm excitation; a Corning 3-72 filter was used to prevent this light from reaching the detection optics. All PL and EL spectra were corrected for detector sensitivity from 350 nm to 800 nm using a procedure previously described (3). The correction factors were incorporated into a computer program for use with an APPLE II Plus Computer. Spectra were digitized, corrected by the program, and plotted on an EPSON printer.

Measurements of $\phi_r$ were made by placing the ZnSe:Al samples and MgO powder (reference) in turn in a quartz cuvette positioned in the Aminco-Bowman spectrometer's sample compartment as previously described (3,12). The sample was irradiated "head-on" with the spectrometer's high-pressure Xe lamp; interference filters (FWHM is $\sim$10 nm except for 366 nm where it is $\sim$30 nm) were used to isolate the desired excitation wavelengths. Both the reflected and emitted intensities were corrected for relative detector response.

The dependence of $\phi_r$ on incident intensity was probed using the near uv lines of a Coherent Radiation CR-12 Ar$^+$ laser (351-and 364-nm doublet). Samples were mounted with epoxy on a glass rod and positioned at $\sim45°$ to both the laser beam and the emission detection optics. PL spectra were run as a function of incident intensity which was varied with Melles Griot neutral density filters; the EG&G radiometer was used to measure incident intensity in conjunction with a glass slide which served as a beam splitter.

Time-resolved PL data were obtained in air with a pulsed $N_2$ laser (337 nm) and $N_2$-pumped dye laser (460 nm) using instrumentation and techniques previously reported (13). Peak intensities of $\sim3$ and 30 kW/cm$^2$ were used in these experiments with essentially no difference in the resulting decay curves.

PEC Experiments. A flat-faced quartz cell equipped with a side arm was employed for most PEC measurements. Long-term stability experiments in diselenide and ditelluride electrolytes were conducted as described previously with an n-ZnSe:Al working electrode and a Pt foil counterelectrode (8). A polyethylene bag was attached to the top of the cell and purged with $N_2$ during the experiments.

Photoaction spectra were obtained as previously described (14) using transparent selenide electrolyte. The output of a 150-W Xe lamp (Oriel) was monochromatized for excitation; lamp intensity was measured with the EG&G radiometer whose response from 350-800 nm was corrected with the manufacturer's calibration factors. Photocurrents were measured at -1.0 V vs. SCE.

A standard three-electrode potentiostatic setup was used for obtaining iLV data. Excitation at 366, 405, and 436 nm (200-W, high-pressure Osram Hg lamp with interference filters) was used; lenses and masks were used to fill the exposed electrode area with light. Electrochemical measurements were made with an EG&G PAR Model 174 potentiostat; i-V curves were recorded on a Houston Model 2000 x-y recorder. Steady-state PL intensity in operating PEC's was influenced by production of colored $Se_2^{2-}$ and $Te_2^{2-}$ species. A pulse technique

was employed to minimize this problem during the generation of iLV curves.
The technique consisted of pulsing the electrode between open circuit and
increasingly positive potentials. Typically, the electrode sat at open circuit
for 500 ms, then was pulsed for 57 ms to a potential which increased by 5 mV with

each cycle. The i-V curves obtained in this manner were identical to steady-state
i-V curves. PL was detected with the EG&G radiometer covered by a 600-nm interference
filter. Output signals were displayed on a Tektronix Model RM503 oscilloscope equipped
with a camera; sweep rates which resulted in potential steps of $\sim$10 mV/s permitted
an entire PL intensity-V curve to be photographed with one exposure of $\sim$2 min.
Incident light intensity was measured by inserting a mirror ($\sim$80% reflectivity)
and reflecting the light into the EG&G radiometer. The weakness of the edge PL
required use of the near-uv lines of the $Ar^+$ laser and the Aminco-Bowman
spectrometer for generation of iLV curves in which both PL bands could be monitored.

EL Properties. EL spectra were obtained in 5M $NaOH/0.1$ M $K_2S_2O_8$ electrolyte by
pulsing the electrode between 0.00 V (8 s) and a potential cathodic of
$\sim$-1.7 V vs SCE (1 s),while slowing scanning the monochromator of the emission
spectrometer (12 nm/min), as described previously (11). At potentials where
they could be obtained, steady-state EL spectra were essentially identical to
those generated by the pulse technique.

Instantaneous EL efficiencies were determined as described previously (3).
The total emitted energy per pulse measured with an EG&G Model 550-3 pulse
integration module was converted to 600-nm photons using the manufacturer's
correction factor at that wavelength.

## Results and Discussion

Single-crystal samples of cubic n-ZnSe doped with Al ($\sim$2 ppm) and having carrier concentrations of $\sim 10^{17}$-$10^{18}$ cm$^{-3}$ were employed in these studies. Sections below describe the PL properties of these solids, their perturbation by PEC parameters, and EL from the solids.

PL Spectra. Near-uv excitation of n-ZnSe:Al crystals produces effulgent, orange emission. The 295 K PL spectrum of the material, Fig. 1, is dominated by a broad band (FWHM $\sim$115 nm) with $\lambda_{max}$ $\sim$600 nm; a weaker, sharper band (FWHM $\sim$10 nm) peaking at $\sim$460 nm is also present. The latter transition, whose intensity is reported to be very sensitive to preparative conditions (15), occurs near the band gap energy ($E_g$ $\sim$2.7 eV (16)). Although the band's origin in our samples is unknown, its designation as edge emission appears apt based on its energetic proximity to $E_g$ and its temperature dependence: Fig. 1 indicates that the band blue shifts by $\sim$0.09 eV to 445 nm upon cooling to 77 K, consistent with the temperature coefficient of $-4.1 \times 10^{-4}$ eV/K reported for exciton emission from cathodo-luminescence studies (16b).

An intense orange band at $\sim$630 nm has been reported for many ZnSe samples and assigned as self-activated (SA) PL; the transition is believed to involve a deep trapping level arising from a complex based on a Zn vacancy, $V_{Zn}$, and a next-neighbor donor impurity such as $Al_{Zn}$ (Al on a Zn site) (17). Our spectra are somewhat more complex, but accord well with spectra reported by Bouley et al (15). Figure 1 reveals that the band at 600 nm seen at 295 K splits into two bands with $\lambda_{max}$ $\sim$630 and 550 nm at 77 K. The former, likely the SA band, has been assigned to complexes involving a neutral $(V_{Zn}Al_{Zn})$ or ionized defect $(V_{Zn}Al_{Zn})^-$, while the latter was ascribed to a defect involving Al and an alkali metal impurity (15). For convenience, we will refer to the 600-nm transition as a SA band, although we emphasize that its origin is not fully established in our samples.

PL Efficiency. As previously noted, samples of n-ZnSe:Al are highly emissive. We have employed a technique to obtain $\phi_r$ values which, using a common geometry, compares light reflected from a nonabsorbing material with light reflected and emitted from a sample (12). Table I presents a compilation of measured $\phi_r$ values obtained in air for the SA emission using several different excitation wavelengths. The tabulated values, uncorrected for self-absorption and internal reflectivity, are substantial, ranging from $\sim$2-5%. Large radiative efficiencies are also supported by the modest doubling of $\phi_r$ observed when samples are cooled to 77 K. Similar efficiencies and thermal behavior were reported for the ZnSe:Al samples studied by Bouley et al (15). The decline in $\phi_r$ with excitation wavelength, Table I, suggests the presence of a nonemissive near-surface region: Reported absorptivities increase substantially below 460 nm (18), so that a nonemissive layer is expected to reduce $\phi_r$ as it absorbs larger fractions of incident light.

PL Decay Times. Time-resolved PL properties were studied in air using the 337- and 460-nm outputs of a $N_2$ laser and $N_2$-pumped dye laser, respectively. Measurements of the edge PL band were limited by the duration of the laser pulse, indicating a decay time of $\lesssim$7 ns. A similar limitation was observed for the rise time of the SA band and its initial decay. After the peak intensity of the band had dropped $\sim$30%, however, a much longer nonexponential decay was observed with typical $\tau_{1/e}$ values being $\sim$ 1 $\mu$s. These properties were independent of the excitation wavelengths employed and of the PL wavelength monitored.

Mechanistically, the different temporal behavior of the edge and SA bands is an important result in that it indicates that the corresponding excited states are not thermally equilibrated (19). Initiation of the SA emission is also addressed by the data. Although the rapid rise time for the SA band could reflect population via the excited state responsible for edge emission, our data are also consistent with population from a yet higher-energy state when ultraband gap wavelengths are employed; in the latter case, the strong lattice

coupling characteristic of deep traps provides a relaxation mechanism for rapid population of the SA state in parallel with population of the state leading to edge emission. Excited-state communication by either of the schemes outlined is also supported by steady-state measurements using the near uv lines of an Ar^{+} laser; over an incident intensity range of $\sim 10^{-2}$ to $10^{1}$ mW/cm$^{2}$, the intensities of the edge and SA PL bands maintain a constant ratio.

PEC Properties. Although n-ZnSe has been used as an electrode in PEC's (18,20), the material has not, to our knowledge, been stabilized to the extent that it can be used for efficient conversion of optical energy to electricity; decomposition according to eq. (1) has previously been observed in several electrolytes (20a,b,f). The ability to stabilize n-CdX (X = S, Se, Te) electrodes with polychalcogenide

$$ZnSe \xrightarrow{h\nu} Zn^{+2} + Se + 2e^{-} \qquad (1)$$
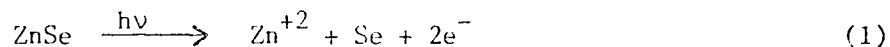
electrolytes suggested their use with n-ZnSe electrodes (9). In an initial experiment with sulfide electrolyte (1M OH$^{-}$/1M S$^{2-}$), decomposition still obtained: photocurrent fell rapidly, and pitting of the surface occurred. However, PEC's constructed from n-ZnSe:Al, a Pt counterelectrode and (di)selenide or (di)telluride electrolyte were stable. Table II demonstrates that little electrode weight loss accompanies long-term experiments in these electrolytes. Other evidence of stability includes relatively constant photocurrents and lack of surface damage in the prolonged experiments, as well as observation of competitive electrolyte oxidation (9).

We obtained photoaction spectra of our samples near short circuit in a transparent selenide electrolyte. Figure 2 reveals that, as expected, photocurrent rises sharply at $\sim 460$ nm, roughly the band gap energy. The enhanced efficiency of e$^{-}$-h$^{+}$ pair separation with decreasing wavelength is consistent with the reported trend in absorptivities (18) and with the decline in electric field strength with distance from the interface (21).

Current-voltage curves, shown in Figure 3, reveal that photocurrent in diselenide electrolyte onsets at ∿-2.0 V vs. SCE at moderate light intensities of ∿10 mW/cm$^2$, yielding an open-circuit voltage of ∿1.0 V. The photocurrent quantum efficiency, $\phi_x$, is relatively low for these PEC's. Table I shows that even the least deeply penetrating wavelength, 366 nm, yields a short-circuit $\phi_x$ value of only ∿0.50. We attribute the low $\phi_x$ values to narrow depletion widths, W, and short hole diffusion lengths, $L_p$, in these materials: W is calculated to be ∿300-1000 Å at short-circuit in our materials (22), and $L_p$ has been reported to be only ∿10$^2$ Å for comparably-doped ZnSe materials (20e). We estimate f ∿m PL data (vide infra) that the 366-nm absorptivity of ZnSe is ∿6-8x10$^4$ cm$^-$ so that a significant fraction of e$^-$-h$^+$ pairs would be created beyond the dept here holes can be collected by diffusion into the drift region. Despite th modest $\phi_x$ values, Table I demonstrates that n-ZnSe:Al-based PEC's can still yield substantial efficiencies for the conversion of monochromatic light to electricity, values of ∿5-7% for 366-nm excitation being typical. In the protracted experiments of Table II, energy conversion efficiencies of ∿3-4% (366-nm experiments) were sustained for several days.

Of particular interest to us are changes in PL properties which accompany the use of the semiconductor as an electrode. Figure 4 demonstrates that in passing from open circuit to short circuit, the two PL bands are quenched roughly in parallel by the applied electric field. The spectral distribution is invariant over the potential range of Figure 3, permitting changes in PL intensity to be monitored at a single wavelength. Simultaneous measurements of current, PL intensity, and potential (iLV) data are illustrated in Figure 3 and summarized in Table I. The table reveals that PL quenching obtains with all of the excitation wavelengths employed.

Quenching of semiconductor PL by applied potential is a well-documented phenomenon in both semiconductor/metal- (6,23) and PEC-based (2,3) Schottky-barrier systems. A dead-layer model which quantifies PL quenching in the solid-state systems has recently been found applicable to PEC's based on n-CdSe and n-GaAs (4,5). In its simplest form, the model states that $e^- - h^+$ pairs formed within some fraction of the depletion width are swept apart by the field and do not contribute to PL. The mathematical form of the model is given by eq. (2) where D

$$\frac{\phi_r}{\phi_{r_{FB}}} = \exp(-\alpha'D) \tag{2}$$

is the dead-layer thickness; $\phi_r$ and $\phi_{r_{FB}}$ are the radiative quantum efficiencies at an in-circuit potential and at flat-band potential (approximated here as the open-circuit potential); and $\alpha' = \alpha + \beta$ with $\alpha$ and $\beta$ the solid's absorptivities for the exciting and emitted light, respectively.

The dead-layer model was recently shown to be applicable to PL from a Au-ZnSe Schottky diode; PL intensity-voltage curves obtained with 442-nm light could roughly be fit by assuming that D has a functional dependence like that of W (D proportional to $(V-V_{FB})^{\frac{1}{2}}$)(6). For the n-ZnSe:Al-based PEC's, PL quenching curves like that shown in Figure 3 can be similarly fit, although discrepancies occur near open circuit. Such discrepancies, also noted for n-GaAs-based PEC's, may indicate that potential applied in this regime is partitioned between the semiconductor and the Helmholtz layer (4).

Another quantitative test of the dead-layer model, independence of D on optical penetration depth, is presently precluded by a lack of reliable absorptivities for n-ZnSe:Al. However, qualitative accord is indicated by the enhanced PL quenching at short circuit with decreasing wavelength and penetration depth, Table I. If the dead-layer model is assumed applicable to these PEC's, it yields, using $\alpha \sim 3 \times 10^4$ cm$^{-1}$ for 436-nm light (6), absorptivities of $\sim 4 \times 10^4$ and $6 \times 10^4$ cm$^{-1}$ at 405 and 366 nm, respectively.

The effect of carrier concentration on PL quenching was also qualitatively consistent with the dead-layer model. As was found in the solid-state study (6), more resistive samples, prepared by heating ZnSe:Al in an evacuated ampule with Se, exhibited greater PL quenching, as shown in Table I. The wider electric fields of these samples were also manifest in larger $\phi_x$ values. Taken as a unit, we believe our data provide good evidence for describing PL quenching in n-ZnSe:Al-based PEC's in terms of a dead-layer model.

A final point of interest concerns the parallel quenching of the two PL bands illustrated in Figure 4. Although we are unable to definitively establish the mechanism for populating the SA state (vide supra), the parallel quenching is consistent with separation of $e^- - h^+$ pairs prior to population of this state.

EL Properties. We have found that n-ZnSe:Al electrodes mimic other II-VI electrodes (3) in exhibiting EL when used as a cathode in aqueous, alkaline, peroxydisulfate electrolyte (24). The key step involved in populating the emissive excited state has been proposed to be hole injection by $SO_4^{\mathbf{\tau}}$ radical anions formed by reduction of $S_2O_8^{2-}$ (25). As in previous studies, we have obtained EL spectra using a pulse technique: while the emission monochromator is swept, the electrode is pulsed repetitively between a potential where no current is observed (0.0 V for 8 s) and a potential sufficiently cathodic to initiate EL (1-s pulse). We find that EL is initiated to the dark-adapted eye at $\sim$-1.7 V vs. SCE, roughly the onset of dark cathodic current in the electrolyte of 5M $OH^-$/0.1 M $S_2O_8^{2-}$.

Figure 5 presents the EL spectrum of an n-ZnSe:Al electrode. Both the edge and SA emission bands are evident, and a comparison with Fig. 1 indicates that the relative intensities of the bands are similar in the two spectra. The overall spectral similarity indicates that the same two emissive excited states are populated in both experiments.

Besides spectral distributions, we have also measured lower-limit integrated EL efficiencies, $\overline{\phi}_{EL}$, using techniques and approximations previously described (3). For n-ZnSe:Al electrodes, we obtain $\overline{\phi}_{EL}$ values of $\sim 10^{-6}$ and $10^{-4}$ at -1.8 and -2.2 V vs. SCE, respectively. These numbers are of interest because $\overline{\phi}_{EL}$ (photons emitted per holes injected) can be factored into an efficiency for excited-state population, $\phi_{ES}$ (excited states populated per holes injected) and the PL radiative efficiency, $\phi_r$ (photons emitted per excited states populated). Samples of $n\text{-}CdS_XSe_{1-X}$ ($0 \le X \le 1$) exhibit $\overline{\phi}_{EL}$ and $\phi_r$ values which are nearly equal, suggesting $\phi_{ES}$ is near unity for these samples. In contrast, our $\overline{\phi}_{EL}$ values for n-ZnSe:Al are lower than the measured $\phi_r$ of $\sim 10^{-1}\text{-}10^{-2}$ by a factor of $10^{-2}\text{-}10^{-4}$. The discrepancy in the two efficiencies may be due to a low value of $\phi_{ES}$ but more likely reflects the different spatial regions involved in the two modes of excited-state population. In particular, EL is expected to originate, on average, from nearer the semiconductor surface than PL, owing to its initiation by interfacial charge transfer. A lower $\phi_r$ value for the (near-)surface region due to nonradiative surface recombination could then account for the observed low EL efficiencies. Such a non-emissive near-surface region has already been suggested to account for the variation of PL efficiency with excitation wavelength. Reduction of the electrode surface during the EL experiment (3) may also contribute to the discrepancy.

## References

1.  (a) A. Heller, <u>Acc. Chem. Res.</u> <u>14</u>, 154 (1981); (b) A. J. Bard, <u>Science</u>, <u>207</u>, 139 (1980); (c) M. S. Wrighton, <u>Acc. Chem. Res.</u> <u>12</u>,303 (1979); (d) A. J. Nozik, <u>Ann. Rev. Phys. Chem.</u> <u>29</u>, 189 (1978).

2.  A. B. Ellis, <u>J. Chem. Ed.</u>, <u>60</u>, 332 (1983) and references therein.

3.  H. H. Streckert, J. Tong, M. K. Carpenter, and A. B. Ellis, <u>This Journal</u>, <u>129</u>, 772 (1982) and references therein.

4.  W. S. Hobson and A. B. Ellis, <u>J. Appl. Phys.</u>, <u>54</u>,5956 (1983).

5.  M. Tomkiewicz, private communication.

6.  K. Ando, A. Yamamoto, and M. Yamaguchi, <u>Jpn. J. Appl. Phys.</u> <u>20</u>, 679 (1981).

7.  O. Lindberg, <u>Proc. of the I.R.E.</u> <u>40</u>, 1414 (1952).

8.  B. R. Karas and A. B. Ellis, <u>J. Am. Chem. Soc.</u> <u>102</u>, 968 (1980).

9.  A. B. Ellis, S. W. Kaiser, J. M. Bolts, and M. S. Wrighton, <u>J. Am. Chem. Soc.</u>, <u>99</u>, 2839 (1977).

10. W. S. Hobson and A. B. Ellis, <u>Appl. Phys. Lett.</u> <u>41</u>, 891 (1982).

11. H. H. Streckert, B. R. Karas, D. J. Morano, and A. B. Ellis, <u>J. Phys. Chem.</u>, <u>84</u>, 3232 (1980).

12. M. S. Wrighton, D. S. Ginley, and D. L. Morse, <u>J. Phys. Chem.</u> <u>78</u>, 2229 (1974). See ref. 3 for previous applications of the technique to semiconductor electrodes.

13. M. M. Olken, R. N. Biagioni, and A. B. Ellis, <u>Inorg. Chem.</u>, <u>22</u>, 000 (1983).

14. M. K. Carpenter, H. H. Streckert, and A. B. Ellis, <u>J. Solid State Chem.</u>, <u>45</u>, 51 (1982).

15. J. C. Bouley, P. Blanconnier, A. Herman, Ph. Ged, P. Henoc, and J. P. Noblanc, <u>J. Appl. Phys.</u> <u>46</u>, 3549 (1975).

16. (a) M. Cardona, *J. Appl. Phys.* 32S, 2151 (1961); (b) B. Sermage, *Solid-State Electron.* 21, 1361 (1978).

17. (a) D. Curie and J. S. Prener in "Physics and Chemistry of II-VI Compounds," M. Aven and J. S. Prener, Editors, Chap. 9.4, North-Holland Publishing Co., Amsterdam (1967) and references therein. (b) S. Iida, *J. Phys. Soc. Jpn.* 25, 177 (1968); (c) G. Jones and J. Woods, *J. Luminescence,* 9, 389 (1974); (d) S. Satoh and K. Igaki, *Jpn. J. Appl. Phys.* 22, 68 (1983).

18. P. Lemasson, A. Etcheberry, and J. Gautron, *Electrochim. Acta,* 27, 607 (1982).

19. (a) B. DiBartolo, "Optical Interactions in Solids," Ch. 18.3, John Wiley and Sons, New York (1968); (b) P. J. Wagner in "Creation and Detection of the Excited State," Part A, Vol. I, A. A. Lamola, Editor, Chapt. 4, Marcel Dekker, New York (1971).

20. (a) R. Williams, *This Journal,* 114, 1173 (1967); (b) J. Gautron, P. Lemasson, F. Rabago, and R. Triboulet, *This Journal,* 126, 1868 (1979); (c) P. Lemasson, J. Gautron, J.-P. Dalbéra, *Ber. Bunsenges. Phys. Chem.* 84, 796 (1980); (d) P. Lemasson, J.-P. Dalbera, and J. Gautron, *J. Appl. Phys.* 52, 6296 (1981); (e) J. Gautron and P. Lemasson, *J. Crystal Growth,* 59, 332 (1982); (f) B. S. H. Royce, F. Sánchez-Sinencio, R. Goldstein, R. Muratore, R. Williams, and W. M. Yim, *This Journal,* 129, 2393 (1982).

21. H. Gerischer, *J. Electroanal. Chem. Interfacial Electrochem.,* 58, 263 (1975) and references therein.

22. A static dielectric constant of 8.7 was used in calculating W, ref. 20d.

23. R. E. Hollingsworth and J. R. Sites, *J. Appl. Phys.,* 53, 5357 (1982) and references therein.

24. EL from n-ZnSe under anodic polarization has also been reported: J. Gautron, J.-P. Dalbera, and P. Lemasson, *Surf.Sci.* 99, 300 (1980).

25. (a) K. H. Beckmann and R. Memming, *This Journal,* 116, 368 (1969); (b) R. Memming, *This Journal,* 116, 785 (1969); (c) B. Pettinger, H. R. Schöppel, and H. Gerischer, *Ber. Bunsenges. Phys. Chem.* 80, 849 (1976).

Table I. PL properties and measurements of efficiency in n-ZnSe:Al-based PEC's[a]

| Electrode[b] | $\lambda_{ex}$, nm[c] | $\Phi_r$[d] | $\Phi_x$[e] | $(1-\frac{\Phi_r}{\Phi_{r_{FB}}})$[f] | $\Phi_x @ \eta_{max}$[g] | $E_v @ \eta_{max}, V$[h] | $\eta_{max}$ (%)[i] |
|---|---|---|---|---|---|---|---|
| as received | 366 | 0.02 | 0.50 | 0.16 | 0.35 | 0.85 | 7.2 |
|  | 405 | 0.03 | 0.25 | 0.11 | 0.18 | 0.85 | 4.9 |
|  | 436 | 0.04 | 0.18 | 0.09 | 0.14 | 0.90 | 4.2 |
|  | 460 | 0.05 |  |  |  |  |  |
| treated | 366 |  | 0.60 | 0.38 | 0.42 | 0.85 | 10.4 |
|  | 405 |  | 0.31 | 0.17 | 0.23 | 0.77 | 5.3 |
|  | 436 |  | 0.22 | 0.13 | 0.13 | 0.73 | 3.6 |

[a]PL properties related to use of n-ZnSe:Al electrodes in PEC's. Most of the properties are derived from iLV curves generated with a three-electrode potentiostatic setup (n-ZnSe:Al working electrode, Pt foil counterelectrode and SCE reference electrode). To optimize transparency, experiments with 366-nm light were conducted in 10M KOH/0.25M $Se^{2-}$/ 0.001 M $Se_2^{2-}$ electrolyte; for 405- and 436-nm light, an electrolyte of 8M KOH/0.2M $Te^{2-}$/0.002M $Te_2^{2-}$ was employed. The electrode, having an exposed surface area of ∿0.25 cm$^2$, was excited with ∿0.5-2 mW of power.

[b]The n-ZnSe:Al sample was used either "as received" or treated with Se as described in the Experimental Section and text.

[c]Excitation wavelength. A 150-W high-pressure Xe lamp or 200-W high-pressure Hg lamp equipped with interference filters was employed for $\Phi_r$ data and iLV curves, respectively.

[d]Radiative quantum efficiencies obtained in air for the SA band. Values are uncorrected for self-absorption and internal reflectivity.

[e]Measured photocurrent quantum efficiency at −1.0 V vs. SCE. Values are uncorrected for solution absorption and reflective losses.

[f]Fractional PL quenching between −1.0 V vs. SCE and the flat-band potential, approximated here as the open-circuit potential. PL intensity was monitored at 600 nm.

[g]Measured photocurrent quantum efficiency at the potential corresponding to maximum optical-to-electrical energy conversion efficiency.

[h]Output voltage at the maximum energy conversion point. The diselenide and ditelluride redox potentials were −0.95 and −1.10 V vs. SCE, respectively.

[i](Maximum electrical power out divided by input optical power) x 100.

Table II. Stabilization of n-ZnSe:Al photoelectrodes[a]

| Exp't. | Electrolyte[b] | Electrode (mol x 10^4)[c] before | after | Electrons[d] (mol x10^4) | Avg i[e], mA | t,h | Output Voltage, V | $\lambda_{ex}$, nm[f] |
|---|---|---|---|---|---|---|---|---|
| 1 | $Se_n^{2-}$ | 0.81 | 0.80 | 2.06 | 0.063 | 87.5 | 0.36 | 366 |
| 2 | $Se_n^{2-}$ | 1.80 | 1.68 | 3.72 | 0.075 | 133 | 0.75 | 366 |
| 3 | $Te_n^{2-}$ | 0.88 | 0.84 | 3.19 | 0.100 | 85.5 | 0.63 | 436 |
| 4 | $Te_n^{2-}$ | 1.25 | 1.23 | 2.46 | 0.055 | 120 | 0.55 | 436 |

[a]All experiments were run under $N_2$ in stirred solutions in a two-electrode PEC (working electrode and Pt foil counterelectrode) in diselenide or ditelluride electrolyte.

[b]Electrolyte compositions are given in Table I. The initially colorless solutions became dark brown and deep purple as $Se_2^{2-}$ and $Te_2^{2-}$ were formed, respectively, during the course of the experiments. Final $Se_2^{2-}$ and $Te_2^{2-}$ concentrations were ~0.002 and 0.004 M, respectively.

[c]Moles of crystal determined by weight before and after photoelectrochemistry. Crystals used in experiments 1, 2, and 3 chipped while being demounted and were not fully recovered. Surface areas were 0.08, 0.18, 0.09, and 0.12 cm$^2$ for the solids of expt's 1-4, respectively.

[d]Moles of electrons in the external circuit determined by integrating photocurrent-time plots.

[e]Average photocurrent passed during experiment; for current densities, divide by the electrode areas given in footnote c.

[f]Excitation wavelength provided by a 200-W high-pressure Hg lamp equipped with interference filters.

# Figure Captions

Figure 1.  Corrected, front-surface PL spectra of n-ZnSe:Al at 295 K (dashed line) and 77 K (solid line).  Both spectra were taken at the same sensitivity (a 100-fold increase in sensitivity was used in scanning the 410-480-nm region).  The sample was excited with identical intensities of 405-nm light without disturbing the experimental geometry.

Figure 2.  Photoaction spectrum for a n-ZnSe:Al-based PEC in optically transparent selenide electrolyte; the electrode was held at -1.0 V vs. SCE. The plotted values of relative photocurrent have been corrected for variation in light intensity as a function of wavelength.  Although the optical pathlength was minimized, the spectrum is not corrected for electrolyte absorption.

Figure 3.  Photocurrent (bottom frame) and PL intensity (top frame) monitored at $\lambda_{max}$ $\sim$600 nm vs. potential for a n-ZnSe:Al electrode excited at 366  nm in 10 M KOH/0.25 M $Se^{2-}$/0.001M $Se_2^{2-}$ electrolyte.  The incident light irradiated the $\sim$0.2-$cm^2$ exposed area of the electrode with $\sim$0.60 mW  of power.  The iLV curves were generated using a pulse technique described in the Experimental Section.  The electrolyte redox potential was -0.95 V vs. SCE,

Figure 4.  Corrected PL spectra of a n-ZnSe:Al electrode excited with the near-uv lines (351, 364 nm) of an $Ar^+$ laser in the diselenide electrolyte of Figure 3. Curves A and B were taken at -2.0 V (open circuit) and -1.0 V vs. SCE, respectively. Both spectra were taken in an identical sample geometry.

Figure 5.  Corrected EL spectra of an n-ZnSe:Al electrode obtained in 5M $OH^-$/0.1M $S_2O_8^{2-}$ electrolyte.  The electrode was continuously pulsed between 0.00 V (8 s) and -2.0  V vs. SCE (1 s) while the emission spectrometer was swept at 12 nm/min.  A 100-fold increase in sensitivity was used in scanning the 400-480-nm spectral region.
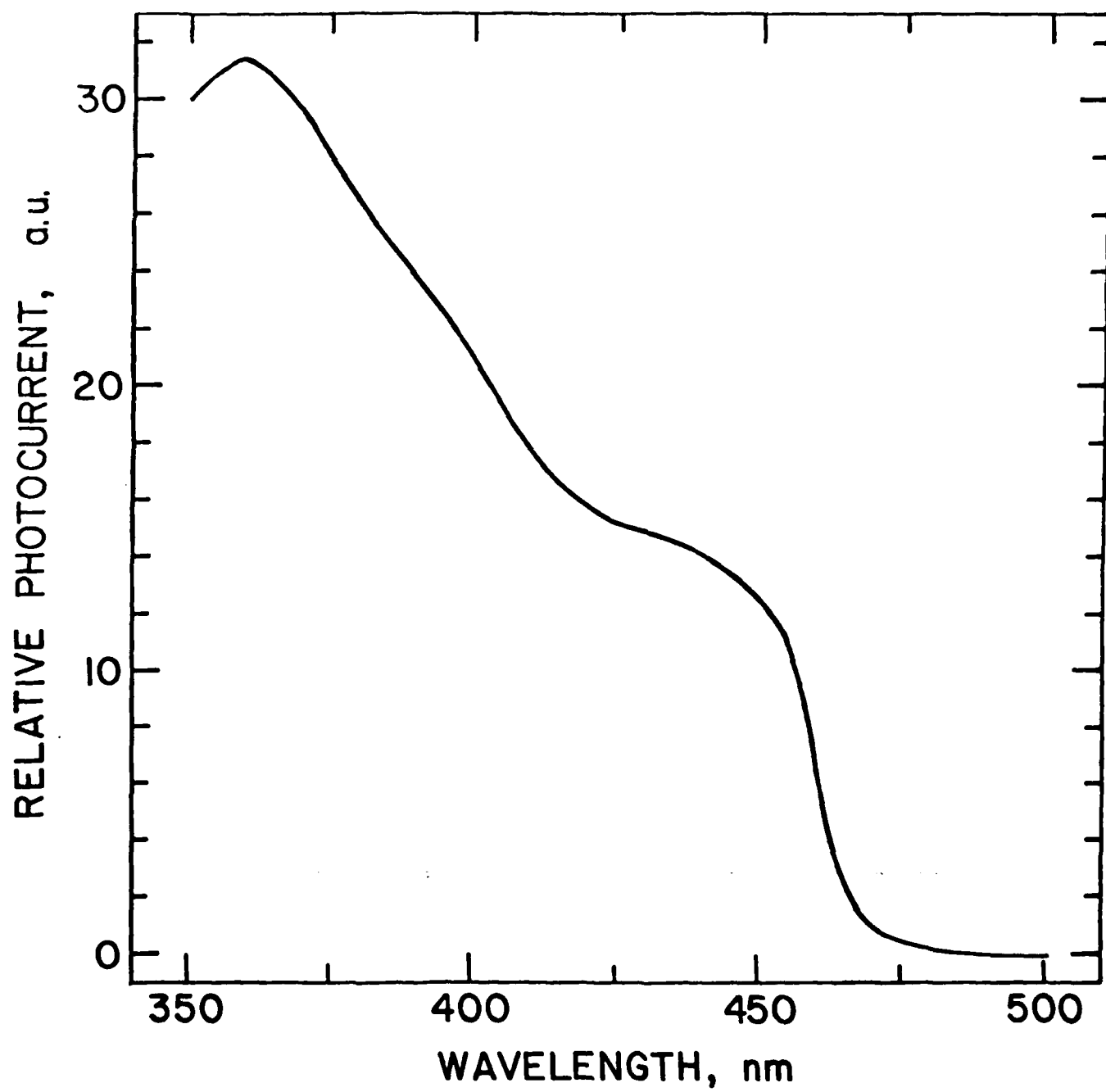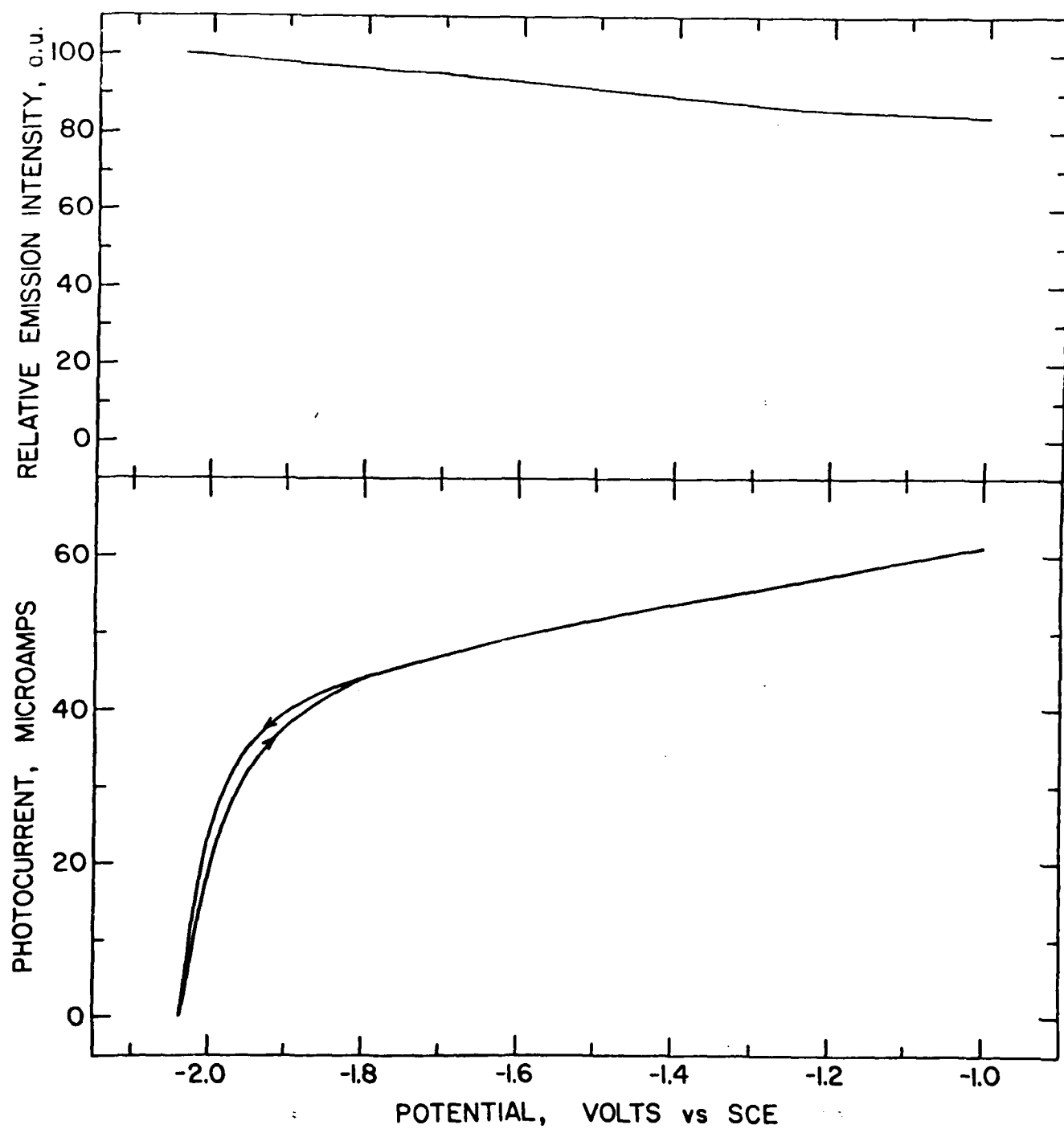
Figure 1    18



RELATIVE EMISSION INTENSITY, a.u.

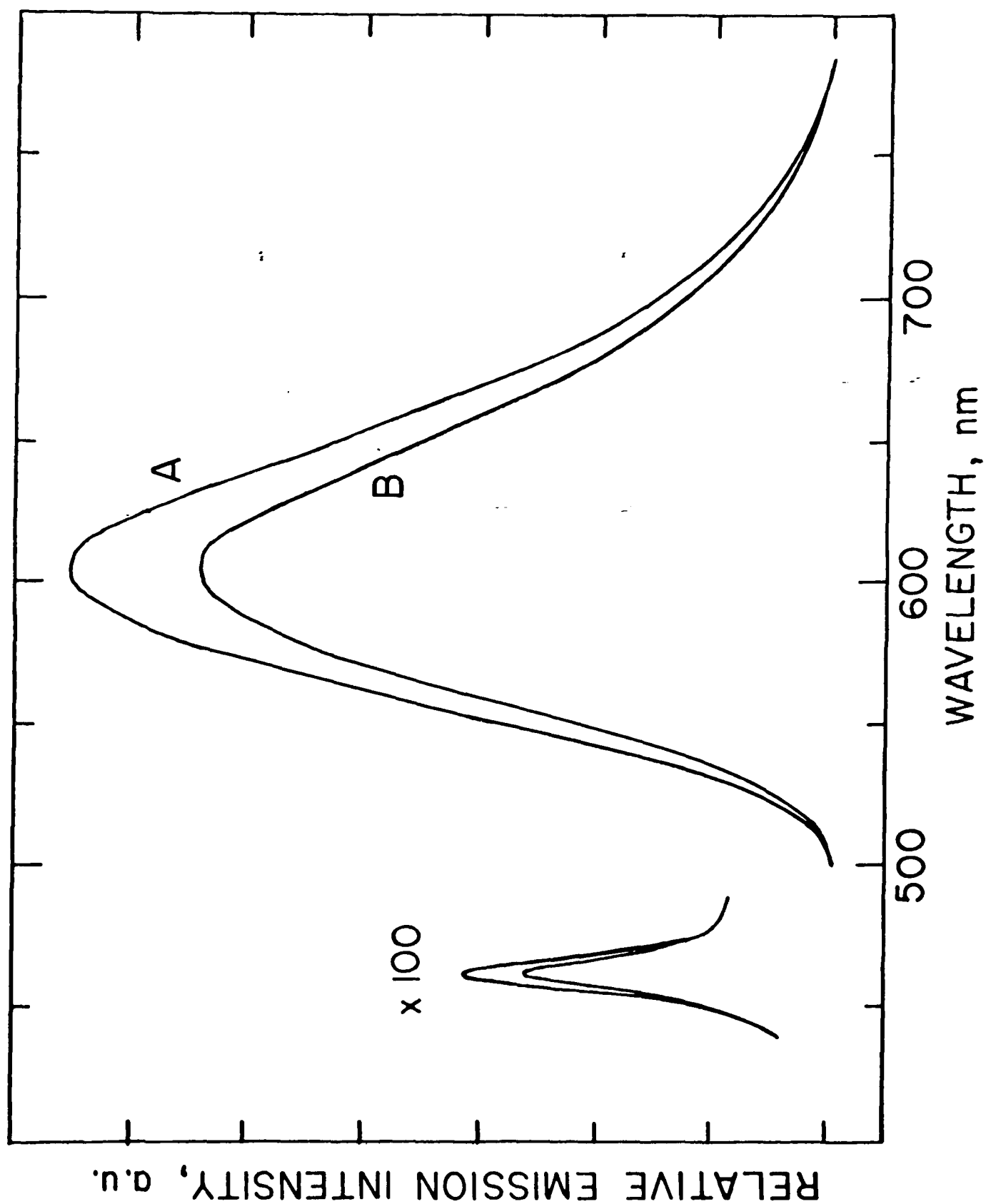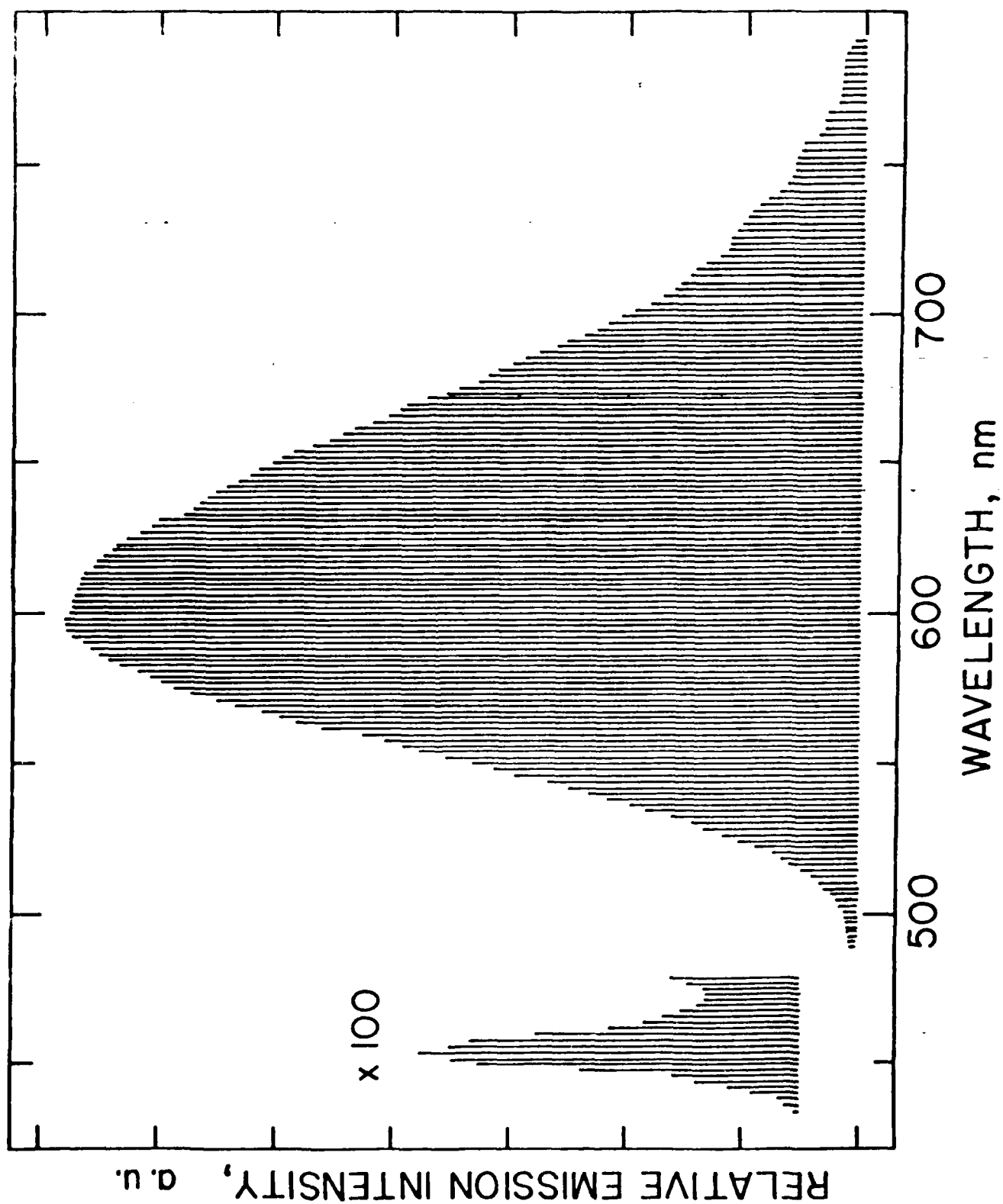WAVELENGTH, nm

x 100

Figure 2    19
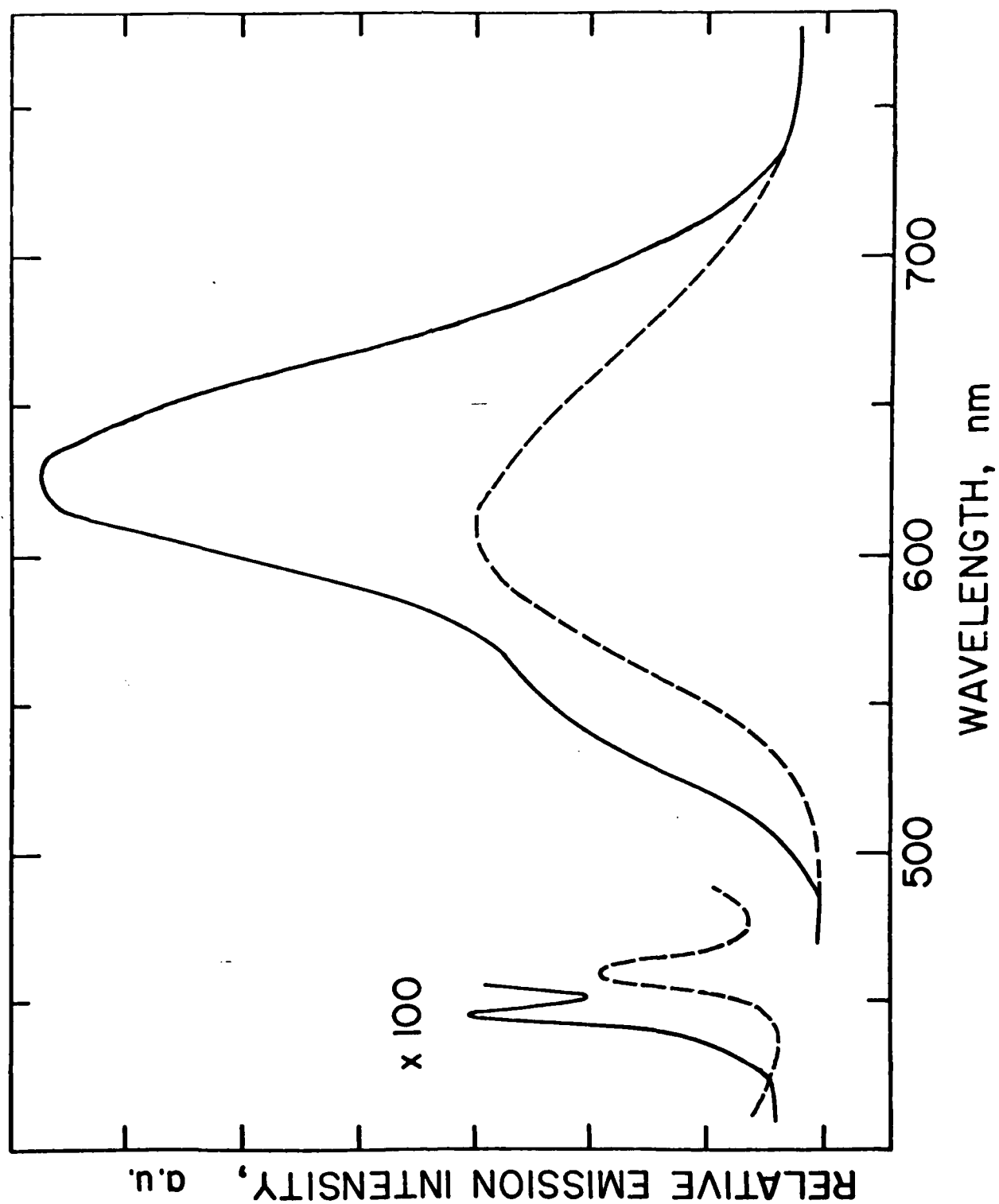
Figure 3

Figure 4

Figure. 5

TECHNICAL REPORT DISTRIBUTION LIST, GEN

No.
Copies

N(
Cop:

Office of Naval Research
Attn: Code 413
300 North Quincy Street
Arlington, Virginia 22217                    2

ONR Pasadena Detachment
Attn: Dr. R. J. Marcus
1030 East Green Street
Pasadena, California 91106                   1

Commander, Naval Air Systems Command
Attn: Code 310C (H. Rosenwasser)
Department of the Navy
Washington, D.C. 20360                       1

Defense Technical Information Center
Building 5, Cameron Station
Alexandria, Virginia 22314                  12

Dr. Fred Saalfeld
Chemistry Division, Code 6100
Naval Research Laboratory
Washington, D.C. 20375                       1

U.S. Army Research Office
Attn: CRD-AA-IP
P. O. Box 12211
Research Triangle Park, N.C. 27709           1

Mr. Vincent Schaper
DTNSRDC Code 2803
Annapolis, Maryland 21402                    1

Naval Ocean Systems Center
Attn: Dr. S. Yamamoto
Marine Sciences Division
San Diego, California 91232                  1

Naval Ocean Systems Center
Attn: Mr. Joe McCartney
San Diego, California 92152

Naval Weapons Center
Attn: Dr. A. B. Amster,
   Chemistry Division
China Lake, California 93555

Naval Civil Engineering Laboratory
Attn: Dr. R. W. Drisko
Port Hueneme, California 93401

Dean William Tolles
Naval Postgraduate School
Monterey, California 93940

Scientific Advisor
Commandant of the Marine Corps
   (Code RD-1)
Washington, D.C. 20380

Naval Ship Research and Development
   Center
Attn: Dr. G. Bosmajian, Applied
   Chemistry Division
Annapolis, Maryland 21401

Mr. John Boyle
Materials Branch
Naval Ship Engineering Center
Philadelphia, Pennsylvania 19112

Mr. A. M. Anzalone
Administrative Librarian
PLASTEC/ARRADCOM
Bldg 3401
Dover, New Jersey 07801

# TECHNICAL REPORT DISTRIBUTION LIST, 359

No.
Copies                                                                    Co

Dr. Paul Delahay
Department of Chemistry
New York University
New York, New York 10003                    1

Dr. E. Yeager
Department of Chemistry
Case Western Reserve University
Cleveland, Ohio 41106                       1

Dr. D. N. Bennion
Department of Chemical Engineering
Brigham Young University
Provo, Utah 84602                           1

Dr. R. A. Marcus
Department of Chemistry
California Institute of Technology
Pasadena, California 91125                  1

Dr. J. J. Auborn
Bell Laboratories
Murray Hill, New Jersey 07974               1

Dr. Adam Heller
Bell Laboratories
Murray Hill, New Jersey 07974               1

Dr. T. Katan
Lockheed Missiles and
  Space Co., Inc.
P. O. Box 504
Sunnyvale, California 94088                 1

Dr. Joseph Singer, Code 302-1
NASA-Lewis
21000 Brookpark Road
Cleveland, Ohio 44135                       1

Dr. B. Brummer
EIC Incorporated
55 Chapel Street
Newton, Massachusetts 02158                 1

Library
P. R. Mallory and Company, Inc.
Northwest Industrial Park
Burlington, Massachusetts 01803             1

Dr. P. J. Hendra
Department of Chemistry
University of Southampton
Southampton SOO 5NH
United Kingdom

Dr. Sam Perone
Chemistry & Materials
  Science Department
Laurence Livermore National Lab.
Livermore, California 94550

Dr. Royce W. Murray
Department of Chemistry
University of North Carolina
Chapel Hill, North Carolina 27514

Naval Ocean Systems Center
Attn: Technical Library
San Diego, California 92152

Dr. C. E. Mueller
The Electrochemistry Branch
Materials Division, Research and
  Technology Department
Naval Surface Weapons Center
White Oak Laboratory
Silver Spring, Maryland 20910

Dr. G. Goodman
Johnson Controls
5757 North Green Bay Avenue
Milwaukee, Wisconsin 53201

Dr. J. Boechler
Electrochimica Corporation
Attn: Technical Library
2485 Charleston Road
Mountain View, California 94040          1

Dr. P. P. Schmidt
Department of Chemistry
Oakland University
Rochester, Michigan 48063                1

## TECHNICAL REPORT DISTRIBUTION LIST, 359

| | No.<br>Copies | | No<br>Copi |
|---|---|---|---|
| Dr. H. Richtol<br>Chemistry Department<br>Rensselaer Polytechnic Institute<br>Troy, New York 12181 | 1 | Dr. R. P. Van Duyne<br>Department of Chemistry<br>Northwestern University<br>Evanston, Illinois 60201 | 1 |
| Dr. A. B. Ellis<br>Chemistry Department<br>University of Wisconsin<br>Madison, Wisconsin 53706 | 1 | Dr. B. Stanley Pons<br>Department of Chemistry<br>University of Alberta<br>Edmonton, Alberta<br>CANADA T6G 2G2 | 1 |
| Dr. M. Wrighton<br>Chemistry Department<br>Massachusetts Institute<br>of Technology<br>Cambridge, Massachusetts 02139 | | Dr. Michael J. Weaver<br>Department of Chemistry<br>Michigan State University<br>East Lansing, Michigan 48824 | 1 |
| Larry E. Plew<br>Naval Weapons Support Center<br>Code 30736, Building 2906<br>Crane, Indiana 47522 | 1 | Dr. R. David Rauh<br>EIC Corporation<br>55 Chapel Street<br>Newton, Massachusetts 02158 | 1 |
| S. Ruby<br>DOE (STOR)<br>600 E Street<br>Providence, Rhode Island 02192 | 1 | Dr. J. David Margerum<br>Research Laboratories Division<br>Hughes Aircraft Company<br>3011 Malibu Canyon Road<br>Malibu, California 90265 | 1 |
| Dr. Aaron Wold<br>Brown University<br>Department of Chemistry<br>Providence, Rhode Island 02192 | 1 | Dr. Martin Fleischmann<br>Department of Chemistry<br>University of Southampton<br>Southampton S09 5NH England | 1 |
| Dr. R. C. Chudacek<br>McGraw-Edison Company<br>Edison Battery Division<br>Post Office Box 28<br>Bloomfield, New Jersey 07003 | 1 | Dr. Janet Osteryoung<br>Department of Chemistry<br>State University of<br>New York at Buffalo<br>Buffalo, New York 14214 | 1 |
| Dr. A. J. Bard<br>University of Texas<br>Department of Chemistry<br>Austin, Texas 78712 | 1 | Dr. R. A. Osteryoung<br>Department of Chemistry<br>State University of<br>New York at Buffalo<br>Buffalo, New York 14214 | 1 |
| Dr. M. M. Nicholson<br>Electronics Research Center<br>Rockwell International<br>3370 Miraloma Avenue<br>Anaheim, California | 1 | | |

TECHNICAL REPORT DISTRIBUTION LIST, 359

| | No.<br>Copies | | No<br>Copi |
|---|---|---|---|
| Dr. Donald W. Ernst<br>Naval Surface Weapons Center<br>Code R-33<br>White Oak Laboratory<br>Silver Spring, Maryland 20910 | 1 | Mr. James R. Moden<br>Naval Underwater Systems<br>Center<br>Code 3632<br>Newport, Rhode Island 02840 | 1 |
| Dr. R. Nowak<br>Naval Research Laboratory<br>Code 6130<br>Washington, D.C. 20375 | 1 | Dr. Bernard Spielvogel<br>U. S. Army Research Office<br>P. O. Box 12211<br>Research Triangle Park, NC 27709 | 1 |
| Dr. John F. Houlihan<br>Shenango Valley Campus<br>Pennsylvania State University<br>Sharon, Pennsylvania 16146 | 1 | Dr. Denton Elliott<br>Air Force Office of<br>Scientific Research<br>Bolling AFB<br>Washington, D.C. 20332 | 1 |
| Dr. D. F. Shriver<br>Department of Chemistry<br>Northwestern University<br>Evanston, Illinois 60201 | 1 | Dr. David Aikens<br>Chemistry Department<br>Rensselaer Polytechnic Institute<br>Troy, New York 12181 | 1 |
| Dr. D. H. Whitmore<br>Department of Materials Science<br>Northwestern University<br>Evanston, Illinois 60201 | 1 | Dr. A. P. B. Lever<br>Chemistry Department<br>York University<br>Downsview, Ontario M3J1P3<br>Canada | 1 |
| Dr. Alan Bewick<br>Department of Chemistry<br>The University<br>Southampton, SO9 5NH England | | Dr. Stanislaw Szpak<br>Naval Ocean Systems Center<br>Code 6343<br>San Diego, California 95152 | 1 |
| Dr. A. Himy<br>NAVSEA-5433.<br>NC #4<br>2541 Jefferson Davis Highway<br>Arlington, Virginia 20362 | | Dr. Gregory Farrington<br>Department of Materials Science<br>and Engineering<br>University of Pennsylvania<br>Philadelphia, Pennsylvania 19104 | |
| Dr. John Kincaid<br>Kaman Sciences Corporation<br>1911 Jefferson Davis Hwy., Suite 1200<br>Arlington, Virginia 22202 | | Dr. Bruce Dunn<br>Department of Engineering &<br>Applied Science<br>University of California<br>Los Angeles, California 90024 | |

TECHNICAL REPORT DISTRIBUTION LIST, 359

No.
Copies

N
Cop

M. L. Robertson
Manager, Electrochemical
   and Power Sonices Division
Naval Weapons Support Center
Crane, Indiana 47522 — 1

Dr. Elton Cairns
Energy & Environment Division
Lawrence Berkeley Laboratory
University of California
Berkeley, California 94720 — 1

Dr. Micha Tomkiewicz
Department of Physics
Brooklyn College
Brooklyn, New York 11210 — 1

Dr. Lesser Blum
Department of Physics
University of Puerto Rico
Rio Piedras, Puerto Rico 00931 — 1

Dr. Joseph Gordon, II
IBM Corporation
K33/281
5600 Cottle Road
San Jose, California 95193 — 1

Dr. Robert Somoano
Jet Propulsion Laboratory
California Institute of Technology
Pasadena, California 91103 — 1

Dr. Johann A. Joebstl
USA Mobility Equipment R&D Command
DRDME-EC
Fort Belvior, Virginia 22060 — 1

Dr. Judith H. Ambrus
NASA Headquarters
M.S. RTS-6
Washington, D.C. 20546 — 1

Dr. Albert R. Landgrebe
U.S. Department of Energy
M.S. 6B025 Forrestal Building
Washington, D.C. 20595 — 1

Dr. T. Marks
Department of Chemistry
Northwestern University
Evanston, Illinois 60201

Dr. D. Cipris
Allied Corporation
P. O. Box 3000R
Morristown, New Jersey 07960

Dr. M. Philpot
IBM Corporation
5600 Cottle Road
San Jose, California 95193

Dr. Donald Sandstrom
Washington State University
Department of Physics
Pullman, Washington 99164

Dr. Carl Kannewurf
Northwestern University
Department of Electrical Engineering
   and Computer Science
Evanston, Illinois 60201

Dr. Edward Fletcher
University of Minnesota
Department of Mechanical Engineering
Minneapolis, Minnesota 55455

Dr. John Fontanella
U.S. Naval Academy
Department of Physics
Annapolis, Maryland 21402

Dr. Martha Greenblatt
Rutgers University
Department of Chemistry
New Brunswick, New Jersey 08903

Dr. John Wassib
Kings Mountain Specialties
P. O. Box 1173
Kings Mountain, North Carolina 28086

No.
Copies

Dr. J. J. Brophy
University of Utah
Department of Physics
Salt Lake City, Utah  84112                1

Dr. Walter Roth
Department of Physics
State University of New York
Albany, New York  12222                    1

Dr. Thomas Davis
National Bureau of Standards
Polymer Science and
  Standards Division
Washington, D.C.  20234                    1

Dr. Charles Martin
Department of Chemistry
Texas A&M University                       1

Dr. Anthony Sammells
Institute of Gas Technology
3424 South State Street
Chicago, Illinois  60616                   1

Dr. H. Tachikawa
Department of Chemistry
Jackson State University
Jackson, Mississippi  39217                1

Dr. W. M. Risen
Department of Chemistry
Brown University
Providence, Rhode Island                   1